Characterization of cellular and extracellular regulators of lymphoid organogenesis in the developing bursa of Fabricius

PhD thesis

Emőke Szőcs

Semmelweis University Doctoral School
Molecular Medicine Division

Supervisor: Nándor Nagy, D.Sc
Official reviewers: Péter Balogh, D.Sc
Zoltán Péter Jakus, Ph.D, Habil.

Head of the Complex Examination Committee:
Attila Mócsai, D.Sc

Members of the Complex Examination Committee:
Elen Gócza, D.Sc
Zoltán Péter Jakus, Ph.D, Habil.

Budapest
2026

1. Introduction

The bursa of Fabricius (BF) is a unique avian-specific primary lymphoid organ that is the central site of B cell development in birds. Chicken BF development can be characterized by two distinct morphogenetic events during embryogenesis, which result in the formation of lympho-epithelial follicle buds capable of supporting B cell proliferation and maturation. Further specification of the epithelio-mesenchymal rudiment into bursal lymphoid follicles relies on immigrating blood-borne cells. Diversification of the B cell antibody repertoire takes place in bursal follicles through repeated somatic gene conversion events, a process that occurs exclusively in bursal lymphoid follicles. Perturbations of the early stages of bursa development highlight its indispensable role in generating the antibody repertoire.

While the function of the medulla in bursal lymphoid follicles is well characterized, the steps of BF organogenesis from the initial induction of epithelial follicle buds to the emergence and regulatory function of the cortical compartment are still not fully understood.

Understanding the complex molecular interactions during embryogenesis that lead to the formation of B cell-specific competent niches is essential for understanding how functional immune cells reach maturity and eventually contribute to the development of more effective stem cell therapies for hematologic disorders.

2. Objectives

The bursa of Fabricius serves as the primary lymphoid organ for avian B cell development, characterized by a complex stromal and cellular microenvironment and unique morphogenetic events during early embryogenesis. Despite having in-depth knowledge of B cell function and cellular interactions, microenvironmental factors that drive B cell development and differentiation require further investigation.

The primary objectives of this thesis are to:

1. Identify the lympho-myeloid stem cells driving the ontogenesis of lymphoid follicles in the bursa of Fabricius
2. Characterize the development, structure, and extracellular microenvironment in the cortex of adult lymphoid follicles

Our specific aims are to:

- Identify the lympho-myeloid and stromal cells that precede B cell precursors in early bursal colonization
- Map the fate of EIV-E12+ cells in lymphoid follicles using embryo manipulation techniques
- Characterize the lymphoid, myeloid, and stromal cells in the cortex of adult lymphoid follicles
- Characterize the expression of tenascin-C in the cortex of lymphoid follicles
- Elucidate the regulatory function of tenascin-C in B cell migration using embryo manipulation techniques and *in vitro* assays

3. Methods

3.1. Animals

Fertilized White Leghorn chicken (*Gallus gallus domesticus*) eggs were obtained from commercial breeders (Prophyl-BIOVO Ltd., Hungary). Transgenic *CSF1R*-eGFP-expressing chicken eggs were obtained from the National Avian Research Facility at The Roslin Institute, University of Edinburgh. For epithelial-mesenchymal recombination experiments, quail (*Coturnix japonica domestica*) eggs were purchased from commercial breeders. For chorioallantoic membrane transplantation fertilized duck eggs (*Anas platyrhynchos domesticus*) were obtained from the National Center for Biodiversity and Gene Conservation, Institute for Farm Animal Gene Conservation, Gödöllő, Hungary.

3.2. Immunohistochemistry

After developmental staging, the bursa of Fabricius (BF) from E9-E13 chicken embryos and 2-8 weeks post-hatch chicken were fixed in 4% paraformaldehyde (PFA) for 1 hour at room temperature. Tissue samples were incubated in 15% sucrose overnight at 4°C, then infiltrated with phosphate-buffered saline (PBS) containing 7.5% gelatine and 15% sucrose for 2 hours at 37°C. Impregnated tissue samples were subsequently embedded in the same 7.5% gelatine medium and snap-frozen at -50°C in 2-methylbutane (Sigma, 78-78-4). Frozen gelatine blocks were sectioned by a Shandon cryotome, and 12 μm cryosections were mounted on poly-L-lysine (Sigma, P8920) coated slides. To visualize the expression of specific antigens, sections were incubated with primary antibodies for 1 hour at room temperature, followed by biotinylated secondary antibodies for 45 minutes and avidin-biotinylated peroxidase complex for 30 minutes (ABC; Vectastain Elite ABC kit, Vector Laboratories, PK-6100). Endogenous peroxidase activity was quenched by 3%

hydrogen-peroxide (Sigma, H1009) in PBS for 10 minutes. The binding sites of the primary antibodies were visualized by 4-chloro-1-naphthol (Sigma, C8890).

3.3. Immunofluorescence

For double immunofluorescence, gelatine-embedded 12 µm cryosections were rehydrated in warm PBS for 10 minutes. Sections were incubated with primary antibodies for 1 hour at room temperature, followed by incubation with Alexa-conjugated fluorescent secondary antibodies for 45 minutes at room temperature. Cell nuclei were counterstained with 4,6-diamidino-2-phenylindole (DAPI; Vector Labs, Burlingame, California). To assess cell proliferation, tissue samples were kept in Dulbeccos's Modified Eagles Medium (DMEM, Sigma, D6429) containing 10 µM 5-ethynyl-20-deoxyuridine (EdU) for three hours prior to fixation with 4% paraformaldehyde (PFA). EdU incorporation was subsequently detected using the Click-iT EdU Imaging Kit (Thermo Fisher, C10337). Sections were analyzed using epifluorescence (Nikon Eclipse E800), confocal laser scanning (Zeiss LSM 780) and stimulated emission depletion (STED; Abberior Expert Line- Nikon Ti2) microscopy. Images were acquired using CellSens and ZEISS ZEN software. Post-processing was performed using ImageJ and Adobe Photoshop CC 2020.

3.4. RNAscope *in situ* hybridization

Expression of the CXCL12 chemokine ligand was detected in isolated bursa of Fabricius from 4-week-old chicken. RNAscope was performed with the RNAscope Fluorescent Multiplex Detection Reagent Kit v2 (Bio-Techne, 323136) using a chicken-specific Gg-CXCL12-C2 probe (Bio-Techne, 458251) according to the manufacturer's protocol. To identify the source of the CXCL12 signal, RNAscope was followed by immunocytochemistry as described above.

3.5. Chorioallantoic membrane transplantation

To map the fate of EIV-E12+ cells within bursal lymphoid follicles, E9 chicken bursa of Fabricius were isolated in PBS containing 5% Penicillin/Streptomycin (Pen/Strep, Sigma, P0781) and transplanted onto the chorioallantoic membrane (CAM) of E11 duck embryos. A small, Y-shaped vessel on the CAM was gently traumatized, and the BF primordia were placed directly onto it to promote engraftment. Eggs were sealed with adhesive tape and incubated at 37°C with 70% humidity for additional 7 and 11 days (n=8).

3.6. Epithelial-mesenchymal tissue recombination experiments

The follicle bud inducing capacity of EIV-E12+ cells was evaluated through a series of quail-chick epithelial-mesenchymal tissue recombination experiments. Briefly, E8 quail BF primordium, E9 chicken BF primordium and E9 chicken hindgut were digested with 0.03% collagenase (Sigma, T1875) in DMEM for 15 minutes at 37°C. Enzymatic activity was blocked by three washing steps in fetal bovine serum (FBS, Sigma, F9665). The BF epithelium was isolated from the mesenchyme using fine forceps. To allow the tissues to adhere recombinants (Experiment 1: quail BF epithelium+chicken BF mesenchyme; Experiment 2: quail BF epithelium+chicken hindgut mesenchyme) were cultured on a layer of 3D-collagen gel matrix (Gibco, A10483). After overnight incubation, the recombinant chimeric tissues were transplanted onto the CAM of E9 chicken then cultured for 9 days. CAM grafts were excised, fixed in 4% PFA and embedded in gelatine for cryosectioning.

3.7. *Shh*-RCAS retrovirus-mediated perturbation

Shh misexpression in the developing chick bursa of Fabricius was performed by injecting 1 µl Shh-RCAS virus into the mesenchymal layer of the bursa of Fabricius of E9 chicken

embryos. Shh-RCAS injected E9 bursa primordia were transplanted onto the chorioallantoic membrane of E9 chicken embryos and cultured *in ovo* for an additional 8 days (n=9). CAM grafts were excised and fixed in 4% PFA for 1 hour at room temperature, embedded in gelatine for cryosectioning.

3.8. *In vitro* B cell migration assay

To determine how different matrix molecules affect B cell migration, E13 bursal folds were dissected and explanted onto tissue culture dishes coated with 20 µg/ml fibronectin (Sigma, F1141) or 10 µg/ml tenascin-C (Sigma, CC115). ECM proteins were diluted in RPMI 1640 (Sigma, R8758) and Petri dishes were incubated at 37 °C for 2 hours. To stimulate emigration of B cells, bursal folds were cultured in RPMI medium containing 5% Pen/Strep and 100 ng/ml CXCL12 (100 ng/ml; R&D Systems, 6448-SD-025) (n=6/experimental setup). Cultures were maintained at 37°C, under 5% CO_2 for 24 hours. Adherent cells were fixed in ice-cold 100% methanol for 20 minutes and immunolabeled to detect CXCR4+ bursal B cells.

3.9. B cell adhesion assay

E18 bursal folds were enzymatically digested with 0.03% collagenase IX (Sigma, C9722) and 2% dispase II (Stem Cell Technologies, 07913) diluted in RPMI 1640 medium (Sigma, R8758-500ML) for 30 minutes at 37°C with gentle agitation. The cell suspension was passed through a 40 µm cell strainer and washed twice in RPMI supplemented with 10% FBS and 5% Pen/Strep. Cells were centrifuged at 1500 rpm for 8 minutes, resuspended in RPMI medium, and seeded at a density of 2×10^5 cells in tissue culture dishes coated with chicken tenascin-C (10 µg/ml) and CXCL12 (100 µg/ml; PeproTech, 250-20A). CXCR4 signaling was inhibited by treatment with the CXCR4 receptor antagonist AMD3100 (Sigma, 239820) at a concentration of 200 µM. Adherent cells were fixed in ice-cold 100% methanol for 20 minutes.

4. Results

4.1. Developmental mechanism of lymphoid follicle formation and characterization of bursal lymphoid follicle inducer cells

To characterize the first incoming cells that colonize the bursa primordium and initiate bursal lymphoid organogenesis, we performed extensive immunostaining with a panel of lymphoid- and myeloid-specific markers and examined the blood-borne colonization of the bursa of Fabricius. Infiltration of the bursal surface epithelium by blood-borne CD45+ cells can be first observed at E10 (Fig. 1A, B). At this developmental stage, CSF1R+ myeloid cells are uniformly scattered in the bursa mesenchyme (Fig. 1C), while chB6+ B cells are very few in number and are restricted to outer mesenchymal regions (Fig.1D). In contrast, the EIV-E12 monoclonal antibody consistently labels cell clusters localized within the surface epithelium (Fig. 1E-G).

To exclude the myeloid origin of colonizing EIV-E12+ cells, we analyzed the formation of follicle buds in *CSF1R*-eGFP embryos between E10-13. Immunostaining for CD45 shows the presence of two distinct populations that can be segregated based on their *CSF1R*-eGFP expression. CD45+/*CSF1R*-eGFP- cells reach the surface epithelium at E10, while a population of CD45+/*CSF1R*-eGFP+ ramified cells is present in the mesenchyme adjacent to the epithelium. EIV-E12 immunostaining confirms that *CSF1R*-eGFP- cells that colonize the surface epithelium express the EIV-E12 antigen. The appearance of EIV-E12+/*CSF1R*-eGFP- cells in the epithelium always precedes *CSF1R*-eGFP+ ramified cell colonization. chB6+ B cells can be first detected within the developing follicle buds at E13.

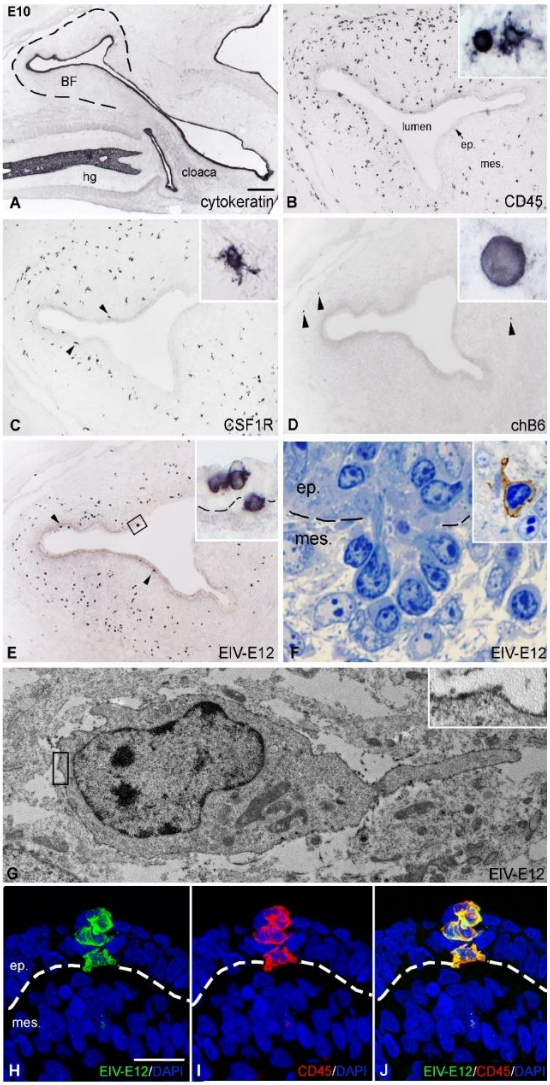


Figure. 1. Initiation of follicle bud formation. (A) The cytokeratin+ epithelial anlage of the BF on E10. **(B)** CD45+ hematopoietic cells are present in large numbers in the bursal mesenchyme. **(C)** CSF1R+ ramified cells are localized in the bursal mesenchyme. **(D)** chB6+ B cell precursors can be first observed on E10. **(E)** EIV-E12+ cells cross the basement membrane of the epithelium and induce follicle bud formation. **(F)** Toluidine blue stained section of darkly stained cells crossing the basement membrane. **(G)** Immunoelectron microscopy of an EIV-E12+ cell **(H-J)** Groups of round EIV-E12+ cells co-express the CD45 common leukocyte antigen and cluster inside the surface epithelium.

4.1.1. EIV-E12+ cells do not give rise to dendritic cells or B cells

To investigate the differentiation potential of the early colonizing EIV-E12+ cells, we performed a chick-duck chimera. Chicken BF rudiments were harvested at E9 and were subsequently transplanted on the chorioallantoic membrane (CAM) of E11 duck embryos. After 7 days of incubation, EIV-E12 immunolabeling confirms that cells have successfully colonized the surface epithelium. After 11 days of incubation, the grafts display several well-differentiated follicles. While initially EIV-E12+ cells were clustered within the surface epithelium, they were later restricted to the interfollicular connective tissue and the follicular medulla. The chimeric follicles lacked donor chicken embryo-derived myeloid and lymphoid cells confirming that leukocyte populations were recruited from the host (duck), rather than differentiating from EIV-E12+ cells already present in the graft.

4.1.2. EIV-E12+ cells induce follicle bud formation

To confirm the inductive role of EIV-E12+ cells, quail-chick epithelial-mesenchymal recombination experiments were performed. In Experiment 1, where quail BF epithelium was recombined with chicken BF mesenchyme, the chimeric graft showed normal folliculogenesis, characterized by the successful recruitment of chicken embryo-derived chB6+ B cells, CSF1R+ dendritic cells, and TIM4+ macrophages into the quail-derived epithelial follicles, confirmed by QCPN positivity (Fig. 2B-F). In contrast, when quail BF epithelium was recombined with chicken hindgut mesenchyme (Experiment 2), which does not harbor EIV-E12+ cells, the grafts failed to develop follicle buds. Although host CD45+ hematopoietic cells infiltrate the hindgut mesenchyme, the absence of EIV-E12+ cells from the hindgut

mesenchyme prevents the differentiation of lympho-epithelial follicle buds from the quail-derived BF epithelium. These findings demonstrate that EIV-E12+ cells are essential drivers of follicle bud initiation within the bursal microenvironment.

4.2. Development of the lymphoid follicular cortex and mechanisms of cortical B cell emigration

4.2.1. Characterization of lymphoid follicles in the chicken bursa of Fabricius

During embryonic development, expansion and maturation of B cells occur within the specialized microenvironment of bursal follicles, which have a central loosely packed medulla and a peripheral, highly dense cortex. While adult lymphoid follicles represent a functional unit, the medulla and the cortex have distinct origins: the medulla develops from the ectoderm, while the cortex is of mesodermal origin. Mesenchymal reticular cells in the cortex co-express vimentin and desmin intermediate filaments. RNAscope *in situ* hybridization further shows that the vimentin+ cortical reticular cells co-express the CXCL12 chemokine. Unlike the medulla, the cortex is rich in extracellular matrix (ECM) proteins. Interestingly, among glycoproteins, tenascin-C exhibits a highly specialized and restricted expression pattern.

4.2.1. Complementary expression of tenascin-C and CXCR4 in the follicular cortex

When we compared the distribution of CXCR4 immunoreactive cells with the expression of tenascin-C, we found that B cells with high CXCR4 expression are localized in outer cortical regions, which are lacking tenascin-C. Similar to

the segregation of CXCR4^{high} and CXCR4$^{low/dim}$ cortical zones, we identified distinct cortical subpopulations based on their mitotic activity. CXCR4^{high} cells are highly proliferative, while CXCR4$^{low/dim}$ cells constitute a quiescent cell population in the tenascin-C-rich inner cortex.

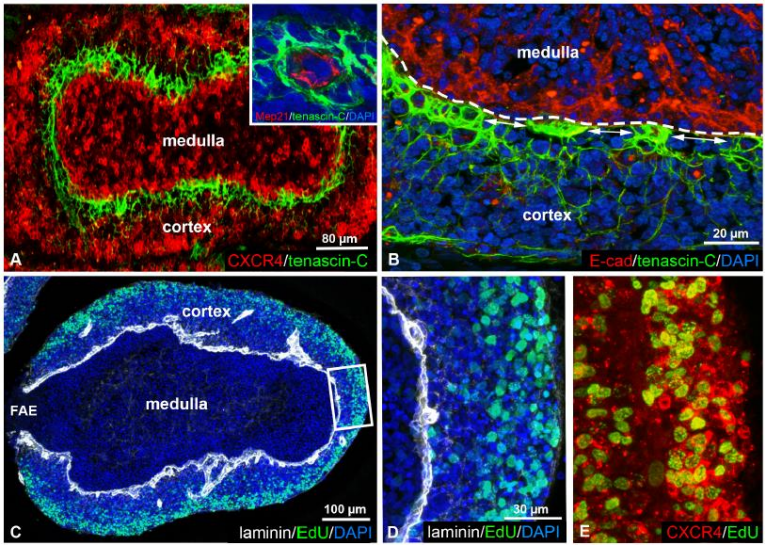


Figure 2. Tenascin-C and CXCR4 show a complementary expression pattern in the follicular cortex.

4.2.2. Shh-induced overexpression of tenascin-C disrupts lymphoid follicle formation

To assess the role of tenascin-C in the earliest stages of bursa development, we utilized the advantages of the avian embryo to experimentally manipulate the bursal mesenchymal environment. Using the same Shh-replication-competent avian retrovirus (RCAS) we overexpressed Shh by injecting E9 BF primordia prior to hematopoietic colonization. This transduction led to the upregulation of tenascin-C expression throughout the

bursa mesenchyme. In Shh-RCAS-injected grafts, the presence of chB6+ B cells is significantly reduced, resulting in the formation of only a few, rudimentary lymphoid follicles. We show that the presence of tenascin-C during bursa colonization inhibits B cell colonization, suggesting that the exclusion of tenascin-C from the cloacal mesenchyme is required for lymphoid follicle colonization.

4.2.3. *In vitro* B cell migration is inhibited by tenascin-C

To assess the inhibitory role of tenascin-C in embryonic B cell migration, we performed *in vitro* migration assays using E13 bursal folds explanted onto the surface of cell culture dishes coated with either 20 ug/ml fibronectin or 10 ug/ml tenascin-C. B cell emigration was stimulated by adding 100 ng/ml CXCL12 to the culture medium. The presence of fibronectin strongly supports the migration of CXCR4+ B cells from the explant. In contrast, the presence of tenascin-C markedly reduced the emigration of CXCR4+ B cells, associated with a round morphology.

Given the fact that tenascin-C possesses conserved motifs for binding CXCL12 we also analyzed the effect of matrix-bound CXCL12 on bursal B cells. In control experiments, isolated bursal B cells seeded on tenascin-C-CXCL12 double-coated surface developed extensive filopodia and long, thin cytoplasmic protrusions. In contrast, blocking CXCR4 function with the receptor antagonist AMD3100, blocked CXCL12-induced cell polarization, and B cells maintained a round, non-polarized morphology. These data indicate that tenascin-C is not only a structural scaffold in the follicular cortex but also functions as a regulatory ECM protein that modulates CXCR4-CXCL12 signaling in the cortical microenvironment.

5. Conclusion

Using avian embryo manipulation and *in vitro* studies, we characterized the ontogeny, cellular architecture, and microenvironmental regulation of lymphoid follicle development in the avian bursa of Fabricius. We also elucidate the spatial organization of the cortical compartment, highlighting how resident stromal cells, extracellular matrix proteins, and chemokines govern B cell migration and compartmentalization.

Our results show that:

- Bursal lymphoid follicle formation is initiated by a novel CD45+/EIV-E12+ blood-borne cell population, which acts as the lymphoid follicle inducer cell during bursal ontogenesis.
- Using embryo manipulation and chick-quail tissue recombination, we demonstrate that EIV-E12+ cells represent a transient, inductive population in the bursa that does not differentiate into dendritic cells, macrophages, or B cells.
- The cortex of bursal lymphoid follicles is supported by a distinct population of desmin+/vimentin+ reticular cells that are the major source of the CXCL12 chemokine in the adult bursa.
- Unlike other ECM proteins, tenascin-C expression first appears in late embryonic stages and is restricted to the inner mesenchymal region in the cortex of adult lymphoid follicles. This distribution creates a complementary expression pattern with CXCR4-immunoreactive cortical B cells.
- Tenascin-C regulates CXCL12-induced embryonic B cell migration *in vitro*.
- *In ovo* Shh-RCAS-retrovirus-induced ectopic tenascin-C overexpression in the embryonic bursa severely disrupts B cell colonization and inhibits lymphoid follicle formation.
- Tenascin-C - CXCL12 interactions control B cell egress from the cortex of bursal lymphoid follicles.

6. Bibliography of the candidate's publications

6.1. List of publications related to the thesis

Szőcs, E., Balic, A., Soós, Á., Halasy, V., and Nagy, N. (2024). Characterization and ontogeny of a novel lymphoid follicle inducer cell during development of the bursa of Fabricius. *Frontiers in Immunology*, 15:1449117. **IF: 5,9**

Soós, Á.*, **Szőcs, E.***, Halasy, V., Jurenka, C., and Nagy, N. (2025). Tenascin-C regulates CXCR4+ B cell migration and cortex formation in the developing bursa of Fabricius. *Frontiers in Immunology*, 16:1636140. *Contributed equally. **IF: 7,0**

6.2. List of own publications not related to the thesis

Roche, D.L.; Naumann, I.; **Szőcs, E.**; Halasy, V.; Kohn, M.; Kaspers, B.; Nagy, N.; Härtle, S. (2026). Characterization of Harderian Gland-Derived Plasma Cells in Chicken. *European Journal of Immunology.* 56(6):70214. **IF: 4,1**

Soós, Á.; **Szőcs, E.**; Halasy, V.; Gecse, Zs.; Mógor, F.; Jurenka, C.; Kocsis, K.; Mucksová, J.; Hejnar, J.; Nagy, N. (2025). Cecal growth factors promote enteric neurosphere formation and hindgut colonization in the avian model. *Frontiers in Cell and Developmental Biology,* 13:1681844. **IF: 5,3**

Dora, D.; **Szőcs, E.**; Soós, Á.; Halasy, V.; Somodi, C.; Mihucz, A.; Rostás, M.; Mógor, F.; Lohinai, Z.; Nagy, N. (2024). From bench to bedside: an interdisciplinary journey through the gut-lung axis with insights into lung cancer and immunotherapy. *Frontiers in Immunology,* 15:1434804. **IF: 5,9**

Molnár, M.; Lázár, B.; Sztán, N.; Végi, B.; Drobnyák, Á.; Buda, K.; Nagy, N.; **Szőcs, E.**; Pecsenye-Fejszák, N.; Liptói, K.; Gócza, E.; McGrew, M.J.; Várkonyi, E. (2024). Successful formation of sperm cells from transplanted primordial germ cells in sterile interspecific avian recipients. *Scientific Reports*, 14(1):24678. **IF: 3,9**

Oláh, I.; Felföldi, B.; Benyeda, Z.; Magyar, A.; Nagy, N.; Soós, Á.; **Szőcs, E.** (2024). Life cycle of chicken bursal secretory dendritic cell (BSDC). *Poultry Science*, 103(6):103640. **IF: 4,2**

Halasy, V.; **Szőcs, E.**; Soós, Á.; Kovács, T.; Pecsenye-Fejszák, N.; Hotta, R.; Goldstein, A. M.; Nagy, N. (2023). CXCR4 and CXCL12 signaling regulates the development of extrinsic innervation to the colorectum. *Development,* 150(8):dev201289. **IF: 3,7**

Kovács, T.*; Halasy, V.*; Pethő, C.; **Szőcs, E.**; Soós, Á.; Dóra, D.; de Santa Barbara P.; Faure, S.; Stavely, R.; Goldstein, A.M.; Nagy, N. (2023). Essential Role of BMP4 Signaling in the Avian Ceca in Colorectal Enteric Nervous System Development, *International Journal of Molecular Sciences,* 24(21):15664. * Contributed equally. **IF: 4,9**

Oláh, I.; Felföldi, B.; Benyeda, Z.; Nagy, N.; Magyar, A.; Szőcs, E.; Soós, Á. (2023). Effect of Intermediate Plus Vaccine and vvIBDV on Bursa Secretory Cells and Their Glycoprotein Production. *Viruses*, 15(6):1301. **IF: 3,8**

Omer, S.; Nagy, N.; **Szőcs, E.**; Kádár, S.; Völgyi, G.; Pinke, B.; Mészáros, L.; Katona, G.; Vincze, A.; Dormán, P.; Nagy Z. Zs.; Balogh G.T.; Kazsoki A.; Zelkó R. (2023). Development of innovative electrospun nepafenac-loaded nanofibers-based ophthalmic inserts. *International Journal of Pharmaceutics,* 647: 23554. **IF: 5,3**

Stavely, R.; Hotta, R.; Guyer, R. A.; Picard, N.; Rahman, A. A.; Omer, M.; Soos, A.; **Szocs, E.**; Mueller, J.; Goldstein, A. M.; Nagy, N. (2023). A distinct transcriptome characterizes neural crest-derived cells at the migratory wavefront during enteric nervous system development. *Development,* 150(5):201090. **IF: 3,7**

Fejszák, N.; Kocsis, K.; Halasy, V.; **Szőcs, E.**; Soós, Á.; Roche, D. L.; Härtle, S.; Nagy, N. (2022). Characterization and functional properties of a novel monoclonal antibody which identifies a B cell subpopulation in bursa of Fabricius. *Poultry Science*, 101(4):101711. **IF: 4,4**

Nagy, N.; Kovács, T.; Stavely, R.; Halasy, V.; Soós, Á.; **Szőcs, E.**; Hotta, R.; Graham, H.; Goldstein, A.M. (2021). Avian ceca are indispensable for hindgut enteric nervous system development. *Development,* 148(22):dev199825. **IF: 6,8**

Σ IF: 68,962